Time dependence of the probability density in the transient regime for tunneling

Gastón García-Calderón
Instituto de Física, Universidad Nacional Autónoma de México, Apartado Postal 20-364, 01000 México D.F., Mexico

Jorge Villavicencio
Facultad de Ciencias, Universidad Autónoma de Baja California, Apartado Postal 1880, Ensenada B.C., Mexico

(Received 16 February 2001; published 15 June 2001)

An exact analytical solution to the time-dependent Schrödinger equation with cutoff wave initial conditions is used to investigate the fast tunneling response of a rectangular potential barrier. We find that just across the tunneling region, the probability density exhibits at short times a transient behavior that may be characterized by a peak t_p and a width Δt. We show that t_p provides the earliest tunneling response of the system and that the top-barrier S-matrix poles play an important role in the process. As a function of the barrier width, t_p exhibits two regimes. Along the first regime, t_p remains almost a constant; as the barrier width increases, a second regime appears where t_p grows linearly with the barrier width.

DOI: 10.1103/PhysRevA.64.012107 PACS number(s): 03.65.Xp, 03.65.Ta, 03.65.Ca, 73.40.Gk

I. INTRODUCTION

Quantum tunneling, which refers to the possibility that a particle traverses through a classically forbidden region, constitutes one of the paradigms of quantum mechanics. In the energy domain, where one solves the stationary Schrödinger equation at a fixed energy E, tunneling is well understood. In the time domain, however, there are still aspects open to investigation. Recent technological achievements, such as the possibility of constructing artificial quantum structures at nanometric scales [1], have stimulated work on time-dependent tunneling both at an applied and a fundamental level.

In this work, we address the issue of the behavior of the time-dependent solution to the Schrödinger equation for tunneling through a potential barrier with cutoff wave initial conditions [2,5–8]. Our problem may be visualized as a *gedanken experiment* consisting of a shutter, situated at $x=0$, that separates a beam of particles from a potential barrier of height V_0 located in the region $0\leqslant x\leqslant L$. At $t=0$, the shutter is opened. The probability density rises initially from a vanishing value and evolves with time through $x>0$. The solution at the barrier edge $x=L$ gives the probability density of finding the particle after a time t has elapsed. Since initially there is no particle along the tunneling region, one can argue that detecting the particle at the barrier edge at time t should provide a time scale for the fast tunneling response of the system. Our approach does not refer to the way in which the tunneling particle traverses or transits through the tunneling region, though it may be related to that issue.

The paper is organized as follows. Section II describes the main features of the formalism to calculate the probability density in the transient regime. In Sec. III, we consider the rectangular potential barrier case and study, in several subsections, the resonant transient regime. Here we emphasize the analysis of the time-domain resonance peak as a function of the barrier parameters, make a comparison of our results with a number of tunneling time definitions, and consider the extension of the approach to cutoff pulses. Finally, Sec. IV contains the concluding remarks.

II. FORMALISM

Our analysis is based on a general formalism developed by García-Calderón [8] for the time-dependent solution to the Schrödinger equation for tunneling through an arbitrary potential $V(x)$ that vanishes outside a region $0\leqslant x\leqslant L$. We consider the reflecting cutoff wave initial condition [9],

$$\psi(x,k;t=0)=\begin{cases} e^{ikx}-e^{-ikx}, & x\leqslant 0 \\ 0, & x>0, \end{cases} \tag{1}$$

which guarantees that the probability density vanishes initially at $x=0$. Note that the initial state is not strictly monochromatic (it extends from $-\infty$ to 0) and hence unavoidably it has a distribution of components around k in momentum space. One then proceeds along lines similar to those discussed in Ref. [8] to derive the time-dependent solution $\psi(x,k;t)$ of the Schrödinger equation for the transmitted region, $x\geqslant L$,

$$\psi(x,k;t)=T(k)M(x,k;t)-T(-k)M(x,-k;t) -\sum_{n}^{\infty} T_n M(x,k_n;t) \quad (x\geqslant L), \tag{2}$$

where the quantities $T(k)$ and $T(-k)$ refer to transmission amplitudes [10], and $T_n=2iku_n(0)u_n(L)\exp(-ik_nL)/(k^2-k_n^2)$ is given in terms of the set of resonant states $\{u_n(x)\}$ and complex poles $\{k_n\}$ of the problem [8,11]. The functions $M(x,\pm k;t)$ and $M(x,k_n;t)$ are defined as

$$M(x,q;t)=\tfrac{1}{2}e^{(imx^2/2\hbar t)}e^{y_q^2}\operatorname{erfc}(y_q), \tag{3}$$

where the argument y_q is given by

$$y_q\equiv e^{-i\pi/4}\left(\frac{m}{2\hbar t}\right)^{1/2}\left[x-\frac{\hbar q}{m}t\right]. \tag{4}$$

 ©2001 The American Physical Society

In Eqs. (3) and (4), q stands either for $\pm k$ or k_n, where the index n refers to a given complex pole. Poles are located on the third and fourth quadrants of the complex k plane. The free case solution to the above problem for a cutoff plane wave was considered by Moshinsky many years ago [2,3]. The solution for the free case with reflecting initial condition reads

$$\psi_0(x,k;t)=M(x,k;t)-M(x,-k;t). \tag{5}$$

Note that the solution given by Eq. (2) involves a term reminiscent of the free case and a resonant sum. We shall refer to the former as the free-type term contribution and to the latter as the resonant contribution. From the analysis given in Ref. [8], one can see that the exact solution satisfies the initial condition, and that at long times it goes into the stationary solution, namely

$$\psi(x,k;t)=T(k)e^{ikx}e^{-iEt/\hbar}. \tag{6}$$

III. MODEL

In order to apply the above ideas, we consider a model that has been used extensively in studies on time-dependent tunneling, namely the rectangular barrier potential, characterized by a height V_0 in the region $0\leqslant x\leqslant L$. To calculate the time-dependent solution $\psi(x,k;t)$ given by Eq. (2), in addition to the barrier parameters V_0, L, and the corresponding incidence energy $E=\hbar^2k^2/2m$, we need to determine the complex poles $\{k_n\}$ and the resonant states $\{u_n(x)\}$ of the system [12]. The S-matrix poles for the rectangular barrier potential may be obtained from the corresponding transmission amplitude $T(k)=4kq\exp(-ikL)/J(k)$, where $q=[k^2-k_0^2]^{1/2}$ with $k_0^2=2mV_0/\hbar^2$. They correspond to the zeros of $J(k)$ in the k plane, namely,

$$J(k)=(q+k)^2\exp(-iqL)-(q-k)^2\exp(iqL)=0. \tag{7}$$

We followed a well-established method to obtain the solutions to the above equation [8]. The resonant states $u_n(x)$ satisfy the time-independent Schrödinger equation of the problem with outgoing boundary conditions [8]. They read

$$u_n(x)=C_n[e^{iq_nx}+b_ne^{-iq_nx}]\quad(0\leqslant x\leqslant L), \tag{8}$$

where $b_n=(q_n+k_n)/(q_n-k_n)$ and C_n may be obtained from the normalization condition [8]

$$\int_0^L u_n^2(x)dx+i\frac{u_n^2(0)+u_n^2(L)}{2k_n}=1. \tag{9}$$

Note that both the complex poles and the resonant states are a function of V_0 and L and hence are a property of the system.

A. The resonant transient regime

To exemplify the time evolution of the probability density, we consider a set of parameters typical of semiconductor artificial quantum structures [1]: $V_0=0.3$ eV, $L=5.0$ nm, $E=0.01$ eV, and $m=0.067m_e$, with m_e the electron mass. Our choice of parameters guarantees that most momentum components of the initial state tunnel through the potential. In Fig. 1, we show a plot of $|\psi|^2$ (normalized to incident flux $J_0=\hbar k/m$) calculated at the barrier edge $x=L$ as a function of time. One sees that $|\psi|^2$ rises as soon as $t\neq 0$ [13], and as time evolves, the probability density exhibits a well-defined maximum, which constitutes the earliest evidence of significant tunneling events in the transient regime, i.e., the first response of the system. This maximum of $|\psi|^2$ corresponds to a transient structure that can be characterized by a peak value t_p and a width Δt; since it appears in the time domain, we have named it *time-domain resonance*. The peak value t_p represents the largest probability of finding the particle at the barrier edge $x=L$, presumably after tunneling through the potential barrier. In our example, t_p is 5.34 fs. We define the width of the distribution, Δt, by the rule of the half-width at half maximum. The distribution is broad, since $\Delta t\approx 2t_p$. We have found that for fixed V_0 and E, and a decreasing L, the width diminishes. The same occurs for fixed E and L, and an increasing V_0; systematically, however, we find $\Delta t>t_p$. Since the time-domain resonance plays an important role in the fast response of the system, we explore the different contributions to the probability density in order to determine the origin of such a structure. In Fig. 2 we show the contribution of the resonant sum in Eq. (2) (dashed line). Note that the resonant sum (it converges here with 3 poles) is the main contribution to the time-domain resonance whereas the free-type term contribution is quite small and varies smoothly with time. Calculations using the absorbing initial condition exhibit a similar behavior. Hence a linear combination of reflecting and absorbing initial conditions should also exhibit it.

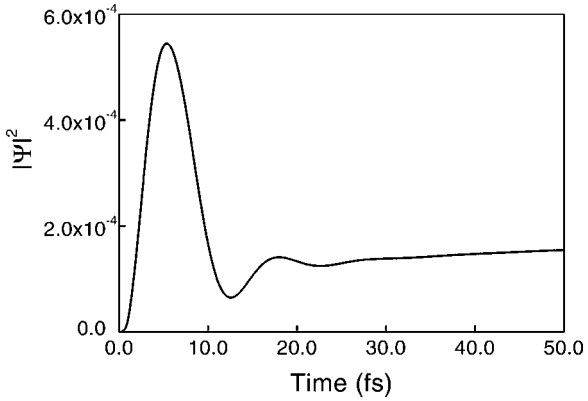

FIG. 1. Plot of $|\psi(L,t)|^2$ as a function of time, for $V_0=0.3$ eV at the barrier edge $x=L=5.0$ nm. At short times, the probability density exhibits a time-domain resonance. See text.

B. Analysis of t_p as a function of the barrier parameters

In Fig. 3, we plot the exact calculation of t_p (solid dots) for different values of the barrier width L. We can clearly identify two regimes. In one of them, t_p remains almost constant as a function of L. This occurs from $L=3.5$ nm up to $L=7.0$ nm. For larger values of L, we have a second regime where the value of t_p increases linearly with L. In the above regimes, the opacity of the system defined as α

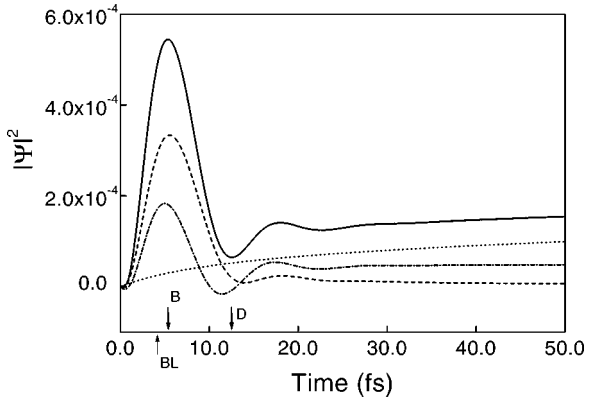

FIG. 2. Plot of $|\psi(L,t)|^2$ at the barrier edge $x=L=5.0$ nm for $V_0=0.3$ eV, as a function of time. Exact calculation (solid line), resonant sum (dashed line), interference term (dashed-dotted line), and free-type term (dotted line) are also shown. See text.

$=([2mV_0]^{1/2}/\hbar)L\equiv k_0L$ is larger than unity, i.e., $\alpha>1$. Not shown in Fig. 3 is a regime that occurs for very shallow or very thin barriers (in our example that occurs for $L<3.5$ nm), characterized by an opacity $\alpha<1$. There the free-type term in Eq. (2) dominates over the resonant sum contribution; consequently, there is no time-domain resonance and the probability density behaves with time in a fashion similar to the free case [2,8].

The linear regime with L in Fig. 3 can be understood from an argument given by Hartman [16]: since the incident wave is not strictly monochromatic, it has momentum components above the barrier height. As the barrier width increases, it reaches a point where those components dominate over the tunneling components. Hartman suggested an approximate traversal time for these components as $t_0\approx L/v_0$, with $v_0=\hbar k_0/m$ and $k_0=[2mV_0]^{1/2}/\hbar$. We obtain a better description by noting that the first top-barrier resonance $k_1=a_1-ib_1$ acts as a filter and hence it favors that only the momentum components close to a_1 traverse above the barrier. This might not hold in general but it does hold in the range

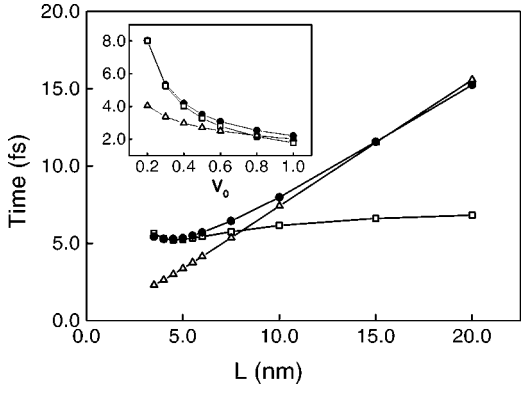

FIG. 3. Plot of an exact calculation for t_p (solid dots) as a function of the barrier width L with the barrier height V_0 fixed. Hollow squares refer to a calculation with $t_p^P=\pi\hbar/(\epsilon_1-E)$ whereas hollow triangles refer to that using $t_p^L=L/v_1$. The inset shows a similar calculation varying V_0 with L fixed. See text.

of large values of L considered. Consequently, in that regime t_p is well described (hollow triangles in Fig. 3) by

$$t_p^L=\frac{L}{v_1}, \tag{10}$$

where $v_1=\hbar a_1/m$ is slightly larger than v_0.

With respect to the plateau regime in Fig. 3, notice, from Fig. 2, that the peak of the resonant sum almost coincides with that of the exact calculation. Note also that the free-type term is small and almost a constant, and that its interference with the resonant term exhibits a similar shape to that of the resonant contribution. It turns out that the main contribution to the sum comes from the first pole term, $E_1=\epsilon_1-i\Gamma_1/2$, and hence one may explore, following [17], the first-term approximation to the probability density using Eq. (2) at $x=L$,

$$|\psi|^2/T\approx 1+e^{-\Gamma_1 t/\hbar}-2e^{-\Gamma_1 t/2\hbar}\cos[\Delta_E t/\hbar], \tag{11}$$

where $\Delta_E=(E-\epsilon_1)$ and T stands for the transmission coefficient. The main contribution to the maximum to the above equation as a function of time is given, to an excellent approximation, by

$$t_p^P=\frac{\pi\hbar}{(\epsilon_1-E)}, \tag{12}$$

which holds provided $(\epsilon_1-E)>\Gamma_1/2$, fulfilled in typical systems. The result of the calculation using Eq. (12) is indicated by the hollow squares in Fig. 3. Surprisingly, it provides an excellent approximation to the exact calculation along the plateau region, even though the other pole contributions have been omitted in the derivation of Eq. (12). Notice that Eq. (12) resembles a time-energy uncertainty relationship, which originates from the interference contribution between the free-type term and the resonant contribution. Hence the time scale t_p^P is not an intrinsic quantity of the system since it depends also on the incidence energy, E, associated to the initial state. In Fig. 3, we exhibit the range of validity of both t_p^L and t_p^P. We have obtained similar results for other sets of potential parameters. The inset to Fig. 3 shows results for an analogous calculation for t_p, t_p^L, and t_p^P by varying the potential height keeping the barrier width fixed ($L=5.0$ nm).

An appropriate form to understand the difference between the plateau and linear regimes discussed previously is to examine the complex top-barrier poles, ϵ_n, as a function of the barrier width L. Figure 4 displays the evolution of the first three values of the real part of ϵ_n, corresponding to the potential barrier of height $V_0=0.3$ eV. Notice that along the plateau region ($3.5\text{ nm}\leq L\leq 7.5$ nm), the energies of the poles are quite separated. In this region, it is easy to convince oneself by inspection of Eq. (12) and by the dramatically different behavior of ϵ_1 (also depicted in the inset) that the first top-barrier pole governs the behavior of t_p observed in Fig. 3. As L increases away from the plateau region, the values of ϵ_n approach essentially the barrier height, V_0.

It is of interest to note that along the plateau regime, the interference between the resonant and the free-type terms is

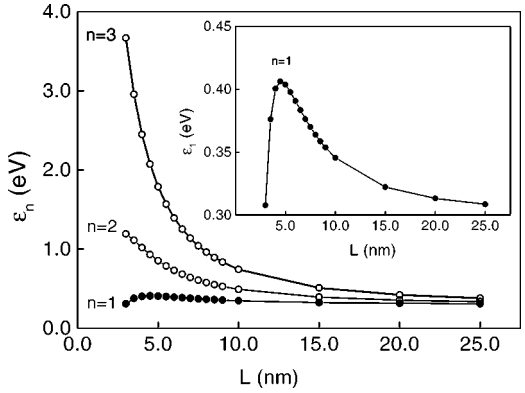

FIG. 4. The real part of the first three top-barrier resonant poles ϵ_n ($E_n=\epsilon_n-i\Gamma_n/2$), corresponding to a potential barrier of height $V_0=0.3$ eV. The main graph shows the evolution of ϵ_n for $n=1,2$, and 3 as a function of the barrier width L. The inset exhibits the peculiar behavior of ϵ_1 (solid dots) in the plateau region (3.5 nm $\leqslant L \leqslant 7.5$ nm). From $L=7.5$ nm onwards, the energies ϵ_n get closer to the barrier height V_0. See text.

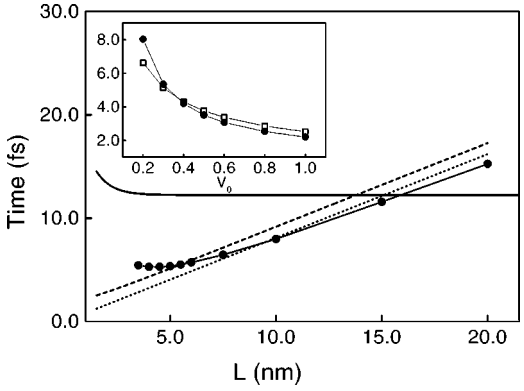

FIG. 6. Plot of an exact calculation for t_p (solid dots) as a function of the barrier width L with V_0 fixed. For comparison, we plot the Büttiker traversal time t_B (dashed line), the semiclassical time t_{BL} (dotted line), and the phase-delay time t_D (solid line). The inset shows a calculation for t_p and t_B varying V_0 with $L=5.0$ nm. See text.

an important contribution (dashed-dotted line in Fig. 2), whereas along the linear regime both the free-type and the interference contributions become negligible as exemplified in Fig. 5 for $L=10$ nm. This is consistent with the discussion given above regarding the behavior of t_p along that regime.

C. Comparison with tunneling time scales

In the literature, one finds a number of definitions of tunneling times attempting to answer the question of the time spent by an incident particle through a tunneling region [18]. As mentioned previously, instead of providing a new definition for the tunneling time, which has become a controversial issue, our approach considers the response time of the system to the tunneling process. In this subsection, we compare our findings with the predictions of a number of definitions of tunneling times. The possible implications of this comparison for the tunneling time problem go beyond the scope of this work and will be considered elsewhere.

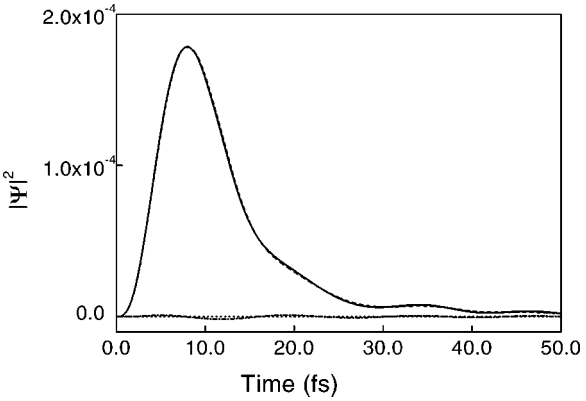

FIG. 5. The time evolution of $|\psi|^2$ (solid line) in the linear regime corresponding to a barrier width $L=10.0$ nm, with $V_0=0.3$ eV and $E=0.01$ eV. As can be seen, the time-domain resonance arises entirely from to the contribution of the resonant sum (dashed line), whereas the contribution of the free-type (dotted line) and interference (dashed-dotted line) terms becomes almost negligible. See text.

Some tunneling time definitions, such as the phase-delay time, are based on a long-time analysis of the solution [16,19] and hence ignore transient effects, as do approaches, at least explicitly, dealing with semiclassical and Larmor times [20]. The arrows in Fig. 2 indicate the values calculated for a number of definitions of tunneling times for the rectangular barrier potential [20], as the semiclassical or Büttiker-Landauer time, t_{BL}; the Büttiker traversal time, t_B; and the phase-delay time, t_D [21]. All of them fall within the broad range of values given by Δt. Note, however, that the Büttiker traversal time t_B is the closest to t_p.

In Fig. 6, we compare systematically the exact calculation for t_p (solid dots), exhibited already in Fig. 3, with exact calculations for t_B (dashed line), t_{BL} (dotted line), and t_D (solid line). One sees that both t_B and t_{BL} are close to the values of t_p, especially along the regime in which it increases linearly with L, where t_{BL} gets closer to t_p. This is not surprising because $t_{\mathrm{BL}}=mL/\hbar q$, with $q=[2m(V_0-E)]^{1/2}/\hbar$ and $q\approx k_0\approx a_1$. However, t_B and t_{BL} do not describe the plateau regime. On the other hand, the phase time t_D exhibits a plateau, though shifted in time from that for t_p. Recalling that t_D follows from a difference between tunneling and free solutions at asymptotically long times, quite differently that for t_p, suggests that both plateaus are unrelated. This deserves further study. It is not surprising that t_D does not reproduce the regime linear with L. This is because the energy involved in its calculation is monochromatic, otherwise t_D would eventually increase linearly with L as discussed above following the argument given by Hartman [16]. The inset exhibits a comparison between the exact t_p (solid dots) and t_B (hollow squares) as a function of barrier height V_0 for fixed barrier width $L=5$ nm. This is a value of L where t_B and t_p are close to each other for $V_0=0.3$ eV and remain so by varying V_0.

It is appropriate to mention here some recent work by Muga and Büttiker [22]. Although these authors consider

both a different system (the step potential) and initial state (frequency-dependent point source), they find a transient behavior in the time dependence of the evanescent probability density characterized by a peak close to but smaller than t_{BL}, in agreement with our Fig. 6 for large values of the barrier width L.

D. Extension to cutoff pulses

In Sec. III A, we mentioned that other types of cutoff initial conditions should exhibit structures similar to the time-domain resonance. In contrast with the *semi-infinite* cutoff plane previously considered, in the present subsection we deal with *finite* cutoff states. In what follows, we discuss the time evolution of *cutoff pulses* and the associated resonant transient response.

Our discussion deals with the solution of the time-dependent Schrödinger equation for a finite range potential $V(x)$ that vanishes outside $0 \leqslant x \leqslant L$, with an initial condition corresponding to a *cutoff pulse* of width a impinging from the left on a reflecting shutter at $x=0$. The condition is given by

$$\psi_p(x,k;t=0)=\begin{cases} 0, & x<-a \\ e^{ikx}-e^{-ikx}, & -a\leqslant x\leqslant 0 \\ 0, & x>0. \end{cases} \tag{13}$$

For the above initial condition, the solution $\psi_p(x,k;t)$ for the transmitted region $(x>L)$ may be obtained along the same lines as discussed in Sec. III; the solution reads

$$\psi_p(x,k;t)=T(k)\mathcal{M}(x,k;t)-T(-k)\mathcal{M}(x,-k;t) - \sum_{n}^{\infty} T_n \mathcal{M}(x,k_n;t) \quad (x\geqslant L). \tag{14}$$

We have introduced the functions $\mathcal{M}(x,q;t)=[M(x,q;t) -(-1)^m M(x+a,q;t)]$, where the M functions are defined by Eq. (3) and the coefficients $T(k)$, $T(-k)$, and T_n are the same as those in Eq. (2). Since the above solution corresponds to a pulse that vanishes exactly at $x=-a$, the initial state must be chosen in such a way that it satisfies the condition $ka=m\pi (m=1,2,3,\ldots)$.

For the sake of comparison with the semi-infinite plane wave in our example we consider the set of typical parameters found in Sec. III A. In this example, we choose $m=9$, which yields a pulse of width $a=213.35$ nm, much larger than the barrier width $L=5.0$ nm, i.e., $a/d=42.67$. The time evolution of the probability density can be appreciated in Fig. 7, where we plot $|\psi_p|^2$ (solid line) as a function of time at the fixed position $x=L$. As can be seen in Fig. 7, the probability density exhibits a time-domain resonance in the short time regime; notice that this structure coincides exactly with the one obtained using a semi-infinite cutoff plane wave (dashed line). The two curves become indistinguishable among them in the short time regime ($t\leqslant 10$ fs). This result is of relevance since it illustrates that the observed behavior is not an artifact of the semi-infinite extension of the cutoff state. For increasing values of time, $|\psi_p|^2$ exhibits a series of oscillations around $|\psi|^2$. As time elapses (not shown here), these rapid oscillations end smoothly at approximately $t \simeq 1.0$ ps; from this value of time onwards, the probability density starts to decrease monotonically reaching vanishingly small values as $t\to\infty$. For pulses of shorter width, a few times the barrier width (not shown), we found that the shape of the time-domain resonance becomes blurred by a series of oscillations.

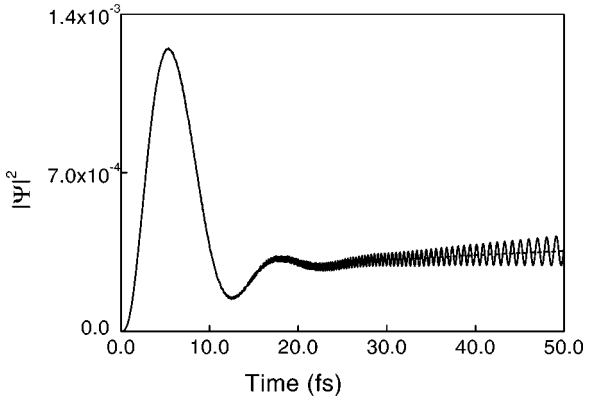

FIG. 7. The time evolution of $|\psi_p|^2$ (solid line) corresponding to a cutoff pulse of width $a=213.35$ nm, at the barrier edge $x=L$. The potential parameters are the same as in Fig. 2. At early times, a time-domain resonance is clearly appreciated. For comparison, a plot of $|\psi|^2$ (dashed line) is also included. Note that both plots are superimposed along the short time regime.

The above results for cutoff pulses suggest that in numerical solutions of the time-dependent Schrödinger equation, where commonly the initial state consists of a Gaussian wave packet initially located far away from the interaction region [23], one would expect to find a time-domain resonance in a plot of $|\psi(L,t)|^2$ vs t, provided (a) the width d of the Gaussian is taken much larger than the barrier width L, i.e., $d\gg L$, (b) the opacity α of the potential, as defined previously, is larger than unity, i.e., $\alpha>1$, and (c) the incidence energy is much less than the barrier height, i.e., $E\ll V_0$.

IV. CONCLUDING REMARKS

Using an analytic dynamical approach involving cutoff semi-infinite waves and extended pulses, a relevant time scale for tunneling has been obtained in the transient regime. We find at short times that the probability density may exhibit a peculiar transient structure called the time-domain resonance. This structure can be characterized by a peak value t_p that governs the fast response of the system. We found that the top-barrier resonant poles and residues play a most relevant role in describing such transient behavior. We have identified two different regimes: the linear regime, occurring at large barrier widths, where tunneling is inhibited and the particle goes over the barrier, and the plateau regime, dominated by the interplay between tunneling and top-barrier resonant processes. We have found simple analytic expres-

sions for the behavior of t_p along the above regimes, given, respectively, by Eqs. (10) and (12). The possible relevance of our results for the tunneling time problem requires further study and will be considered elsewhere. The formalism applies to arbitrary potential barriers and hence we expect our results to hold provided the cutoff initial state is much broader than the barrier width and also that in the exact time-dependent solution given by Eq. (2) the resonant sum dominates over the free-type term.

ACKNOWLEDGMENTS

The authors are indebted to Roberto Romo for fruitful discussions. G.G-C. thanks Gonzalo Muga for useful discussions and M. Büttiker for exchange of correspondence. He also acknowledges the support of DGAPA-UNAM under Grant No. IN116398. The authors acknowledge partial financial support of Conacyt under Contract No. 431100-5-32082E.

[1] E. E. Mendez, in *Physics and Applications of Quantum Wells and Superlattices*, edited by E. E. Mendez and K. Von Klitzing (Plenum, New York, 1987), p. 159.

[2] M. Moshinsky, Phys. Rev. **88**, 625 (1952).

[3] Moshinsky showed that both the probability density and the current, for a fixed value of the distance x_0 as a function of t, present oscillations near the wavefront situated at $t_0=x_0/v$, where $v=\hbar k/m$ stands for the particle velocity. The oscillations constitute a transient regime that he named diffraction in time. Recently, observations of that phenomenon have been reported [4].

[4] P. Szriftgiser, D. Guéry-Odelin, M. Arndt, and J. Dalibard, Phys. Rev. Lett. **77**, 4 (1996); Th. Hils, J. Felber, R. Gähler, W. Gläser, R. Golub, K. Habicht, and P. Wille, Phys. Rev. A **58**, 4784 (1998).

[5] K.W.H. Stevens. J. Phys. C **16**, 3649 (1983).

[6] P. Moretti, Phys. Rev. A **46**, 1233 (1992).

[7] S. Brouard and J.G. Muga, Phys. Rev. A **54**, 3055 (1996). This work deals essentially with the same problem as in Ref. [6], though it considers a different treatment and scope.

[8] G. García-Calderón and A. Rubio, Phys. Rev. A **55**, 3361 (1997).

[9] J. Villavicencio, Ph.D. thesis (unpublished).

[10] The transmission amplitudes $T(k)$ and $T(-k)$ arise, respectively, from the time evolution of the components $\exp(ikx)$ and $\exp(-ikx)$ of the cutoff initial state. In particular, $T(-k)$ satisfies the relationship $T(-k)=T^*(k)$.

[11] G. García-Calderón and R.E. Peierls, Nucl. Phys. A **265**, 443 (1976).

[12] For the rectangular potential barrier, Ref. [7] considers a cutoff initial condition that provides a time-dependent solution that involves a different decomposition in terms of M functions. This approach, and another one using a decomposition closer to Eq. (2), derived by G. García-Calderón, J. L. Mateos, and M. Moshinsky (unpublished), do not consider the useful notion of resonant states.

[13] The probability density increases initially linearly with t [14,15].

[14] See, for example, V. Delgado and J.G. Muga, Ann. Phys. (N.Y.) **248**, 122 (1996).

[15] G. García-Calderón, A. Rubio, and J. Villavicencio, Phys. Rev. A **59**, 1758 (1999).

[16] T.E. Hartman, J. Appl. Phys. **33**, 3427 (1962).

[17] J. Villavicencio and R. Romo, Appl. Phys. Lett. **77**, 379 (2000).

[18] E.H. Hauge and J.A. Stovneng, Rev. Mod. Phys. **61**, 917 (1989); R. Landauer and Th. Martin, *ibid.* **66**, 217 (1994).

[19] F. Smith, Phys. Rev. **118**, 349 (1960).

[20] M. Büttiker, Phys. Rev. B **27**, 6178 (1983).

[21] See, respectively, Eqs. (1.4), (1.7), (3.12), and (3.2) of Ref. [20].

[22] J.G. Muga and M. Büttiker, Phys. Rev. A **62**, 023808 (2000).

[23] A.P. Jauho and M. Jonson, Superlattices Microstruct. **6**, 303 (1989); J.A. Stovneng and E.H. Hauge, Phys. Rev. B **44**, 13 582 (1991); S. Brouard, R. Sala, and J.G. Muga, Phys. Rev. A **49**, 4312 (1994).